DWDM-based effective group velocity dispersion module for long-distance quantum communication

Jin-Woo Chae, Heebong Seo, and Yoon-Ho Kim

***Abstract*—Quantum states of light can be used to encode quantum information, and it can be transmitted over free-space or optical fibers for long-distance quantum communication. Since quantum signals or qubits cannot be amplified, long-distance quantum communication often requires pre-conditioning or preparation of the quantum states for a specific group velocity dispersion (GVD) of the desired fiber-optic channel, which is often difficult experimentally. Moreover, in entanglement-based quantum communication, GVD can be used as another degree of freedom to certify an entanglement signature. However, introducing and controlling large GVD with minimal loss is a challenging problem. In this work, we demonstrate a fiber-optic module capable of introducing a desired amount of GVD to the quantum signal and verify its operation using an entangled photon pair at the telecom wavelength. Our GVD module is based on dense wavelength-division multiplexing (DWDM) technology, and it can be easily designed and operated for various quantum communication scenarios, making it a valuable tool in implementing long-distance quantum communication in varying real-world conditions.**

***Index Terms*—Quantum communication, group velocity dispersion, wavelength-division multiplexing.**

I. Introduction

Group velocity dispersion (GVD) is a fundamental optical phenomenon arising from wavelength dependence of group velocity of light. In optical communication, dispersion introduces challenges such as temporal broadening and distortion of optical pulses, which cause degradation of system performance. Traditionally, dispersion in optical communication has been regarded as a detrimental factor, leading to research efforts focused on mitigating its impact [1]. However, in quantum optics, dispersion emerges as a promising tool to explore quantum phenomena beyond classicality. Nonlocal features of entangled photon pairs can be verified utilizing dispersion. An entangled photon pair generated by a spontaneous parametric down-conversion (SPDC) process, which satisfies the principle of energy conservation, exhibits strong temporal correlations that cannot be explained by local theory [2]. This temporal correlation of the entangled photon pair, which is separated nonlocally and traverses a dispersive media, is utilized in verifying various nonlocal phenomena, such as quantum entanglement sources [3]–[5], quantum communication protocols [6], [7], and quantum key distribution [8]–[10].

In quantum optics, three dispersive media are primarily utilized to induce dispersion: diffraction grating, prism, and optical fiber. Diffraction grating and prism induce dispersion by introducing different optical path lengths for different wavelengths [11], [12], but these methods have limitations regarding the amount of dispersion that can be induced [13]. Optical fibers can be used to induce large amounts of dispersion by extending their length, but optical loss increases correspondingly [14]. Hence, in quantum communication employing optical fiber, where an erbium-doped fiber amplifier (EDFA) cannot be employed due to the no-cloning theorem [15], [16], the length of optical fiber is typically limited to lengths of several tens of kilometers [14], spreading optical pulse with a 10 nm bandwidth to only approximately 10 ns. Consequently, verifying nonlocal features that require stretching an optical pulse over tens of nanoseconds in the time domain is practically unfeasible due to these limitations in the current methodology [17]. Therefore, it is imperative to innovate and develop alternative approaches capable of effectively manipulating the GVD of quantum states.

In this article, we introduce a dispersive medium utilizing dense wavelength-division multiplexing (DWDM) technology capable of generating a GVD equivalent to optical fibers spanning several hundred kilometers or more with minimal optical loss. The DWDM GVD module effectively induces GVD, stretching an optical pulse in the time domain with 10 ps accuracy. We demonstrate that our DWDM GVD module, which has an insertion loss of 4.67 dB, can spread an optical pulse to approximately 85 ns. This corresponds to the dispersion of a typical optical fiber over 379 km with an insertion loss of 75.8 dB (assuming attenuation of 0.2 dB/km), excluding the coupling losses. We anticipate that our work will open up possibilities for introducing new methodologies in applications requiring substantial amounts and precise control of dispersion, such as nonlocal dispersion cancellation [13], [17], [18] and quantum interference [19], [20].

II. Dense wavelength-division multiplexing group velocity dispersion module

We now elaborate on the methodology of the DWDM GVD module. Figure 1(a) shows the basic filtering process of the DWDM filter in our experimental setup, which divides the optical signal traveling through the common port into two ports: the pass port and the reflection port. The optical signal that is transmitted through the DWDM filter propagates via the

This work was supported in part by the National Research Foundation of Korea (RS-2023-00208500), the Information Technology Research Center support program (IITP-2022-RS-2022-00164799), and the National Research Council of Science & Technology (CAP22051-201). (Corresponding author: Yoon-Ho Kim.)

Jin-Woo Chae, Heebong Seo, and Yoon-Ho Kim are with the Department of Physics, Pohang University of Science and Technology (POSTECH), Pohang 37673, Korea. (e-mail: koreacjw@postech.ac.kr; hbseo@postech.ac.kr; yoonho72@gmail.com)

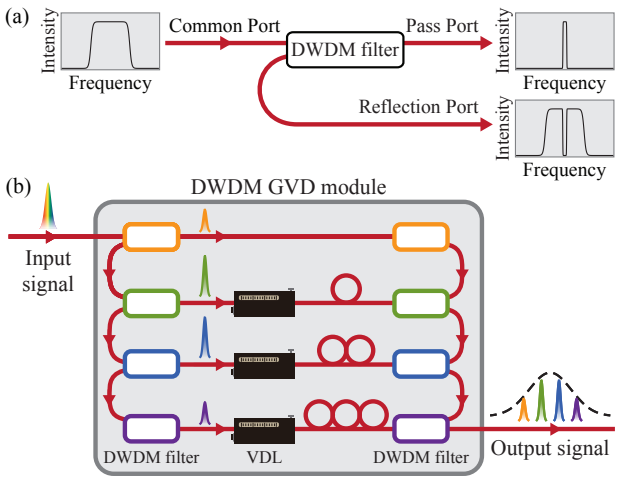

Fig. 1. (a) The spectra of the optical signal as it enters the common port of the 3-port dense wavelength division multiplexing (DWDM) filter and propagates via the pass port and reflection port. The DWDM filter separates the signal, with the transmitted signal propagating via the pass port and the remaining signal via the reflection port. (b) DWDM group velocity dispersion (GVD) module methodology. The color of each DWDM filter represents four different center wavelengths and each circle represents an optical fiber designed to create a constant path length difference. VDL: optical variable delay line.

pass port, while the remaining propagates via the reflection port. Figure 1(b) illustrates the scheme for constructing the DWDM GVD module using DWDM filters with four different center wavelengths, which are arranged with equal spacing between their center wavelengths to ensure consistent spectral intervals. Each optical path length is engineered to have a constant difference with neighboring paths, achieved through fusion splicing of optical fiber with a resolution on the order of tens of picoseconds. Additionally, fine-tuning is achieved through a variable delay line (VDL) with sub-picosecond resolution. In this process, the amount of dispersion is analyzed by measuring the temporal intervals between photons passing through each path.

III. Experiment

We now elaborate on our experimental procedure to verify the performance of a DWDM GVD module. Let us first describe the quantum light source employed for the experiment. We utilize an entangled photon pair generated through an SPDC process. The quantum state of the entangled photon pair can be expressed as [2]

$$|\psi\rangle = \int d\omega_1 d\omega_2 S(\omega_1, \omega_2) a^\dagger(\omega_1) a^\dagger(\omega_2) |0\rangle , \qquad (1)$$

where S represents the two-photon joint spectral amplitude, $\omega_{1(2)}$ denotes the wavelength of the signal (idler), and $a^\dagger$ is the creation operator. In the experiment, the entangled photon pairs are generated by a type-0 SPDC process in a periodically poled lithium niobate (PPLN) crystal pumped by a second harmonic of a picosecond mode-locked fiber laser repeated at 18.02 MHz. The entangled photon pairs exhibit a broad spectral bandwidth of up to 80 nm, centered at 1552.52 nm [21]. The two-photon correlation time of our broadband source, filtered by coarse wavelength-division multiplexing (CWDM) filter with a 3 dB transmission bandwidth of 13.6 nm (1553.25∼1566.85 nm), can be calculated to be approximately 379 fs, assuming the CWDM filter has a Gaussian-shaped spectral function [22].

Initially, the measurement accuracy on temporal differences between arrival times of photons propagating through each path of the DWDM GVD module must be confirmed to measure the amount of dispersion induced. In conventional dispersion experiments, pulse width measurement can be used to verify the amount of dispersion. However, since the DWDM GVD module effectively induces dispersion by optical path length differences among DWDM filters, the temporal difference between the arrival times of photons propagating through each path of DWDM filters is required to obtain the amount of dispersion. The resolution of the time-correlated single photon counting (TCSPC), which measures the temporal differences between arrival times of photons propagating through each path, is in the order of picoseconds, which is bigger than the resolution of fine-tuning on optical path length difference. Therefore, before conducting dispersion experiments using the DWDM system, we assess how precisely temporal differences can be measured under various TCSPC conditions.

Figure 2 shows the experimental setup to confirm the measurement accuracy of the temporal position of the peak from coincidence measurement of entangled pair. The entangled photon pairs generated by the SPDC process are separated into the signal and idler photons by the CWDM filter. Subsequently, after the signal photons pass through a 100 GHz DWDM filter (Flyin, 100G 1×2 DWDM device) of channel

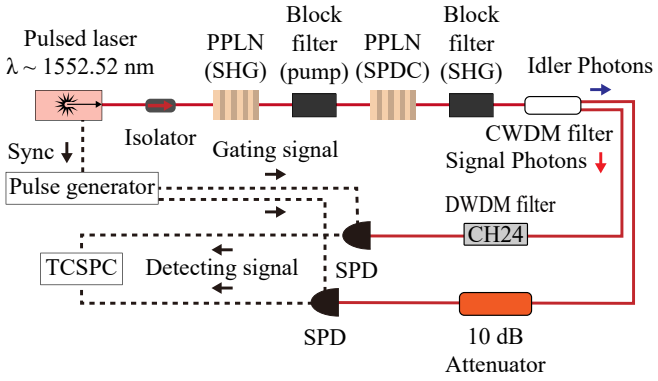

Fig. 2. Experimental setup to confirm the measurement accuracy of the temporal position of the peak from coincidence measurement. The energy-time entangled photon pairs are prepared from periodically poled lithium niobate (PPLN) crystals with a mode-locked picosecond fiber laser. The photon pairs generated from PPLNs are divided into the signal and the idler paths through coarse wavelength-division multiplexing (CWDM) filter. The wavelength range for the signal photons is centered at 1560 nm with a 3 dB bandwidth of 13.6 nm, while the idler photons occupy the rest of the spectrum. Subsequently, the signal photons and idler photons pass through a 100 GHz DWDM filter (Flyin, 100G 1X2 DWDM Device) on channel 24 and a 10 dB attenuator to prevent damage to the detector, respectively, and are detected by an InGaAs single-photon detector (SPD). In our experimental setup, the channel number of DWDM filters follows the ITU grid specification for the telecom C-band 100 GHz grid. The temporal correlation between the signal photons and the idler photons is analyzed using a time-correlated single photon counting (TCSPC) technique. SHG: second-harmonic generation; SPDC: spontaneous parametric down-conversion. CH24: DWDM filter of channel 24, which has a center wavelength of 1558.17 nm, 0.5 dB bandwidth of 0.5 nm, and a flat-top filter shape.

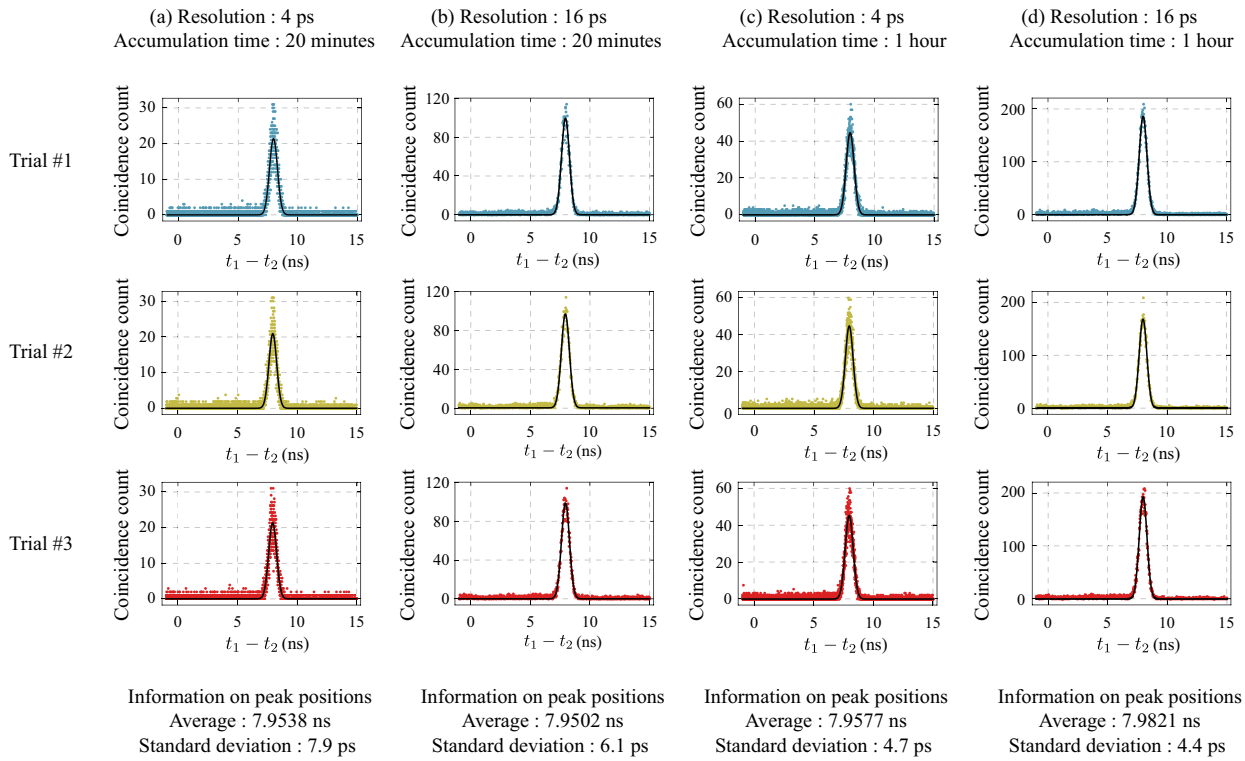

Fig. 3. Experimental results for confirming the measurement accuracy on peak position under various conditions. (a) and (b) show the results obtained with an accumulation time of 20 minutes, each measured with resolutions set to 4 and 16 ps, respectively. (c) and (d) show results using the same method, but the accumulation time is extended to 60 minutes. The information on peak positions below represents the averaged results of peak positions in three trials.

24, which has a center wavelength of 1558.17 nm, 0.5 dB bandwidth of 0.5 nm, and a flat-top filter shape, the entangled photon pairs are detected by InGaAs-based single-photon detectors (AUREA Technology, SPD-A-NIR) operated in gated mode with an extra 10 μs dead time. The temporal correlation between the signal and the idler photon is analyzed using TCSPC (PICOQUANT, PicoHarp300) after the detection. Note that the channel number of the DWDM filters follows the ITU grid specification for the telecom C-band 100 GHz grid. As the signal photons are filtered by 100 GHz DWDM filters, a 10 dB attenuator is installed in the path of idler photons to prevent damage to the detector. To assess the measurement accuracy of the temporal position of the peak, we repeatedly conduct coincidence measurements between photons of the entangled pair under four conditions. Figure 3 illustrates the experimental results of the measurement accuracy on the temporal position of the peak. After conducting measurements three times under each of the four conditions, we confirm that the accuracy of peak position measurement is consistently within 10 ps regardless of the measurement conditions. Consequently, we standardize the TCSPC resolution to 16 ps for all subsequent experiments, adjusting accumulation times based on single-photon counts.

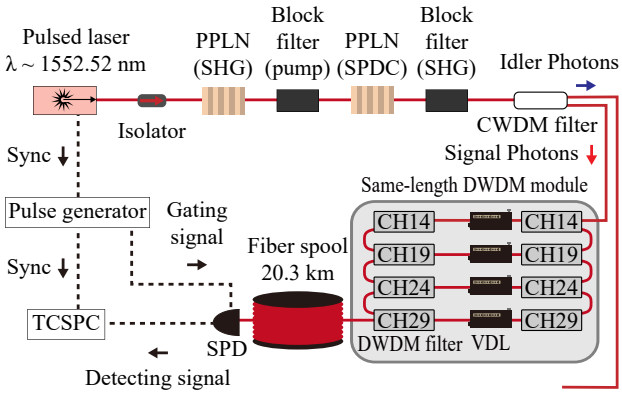

Fig. 4. Experimental setup for measuring the amount of dispersion induced by the fiber spool. The signal photons are detected by the SPD after passing through the same-length DWDM module and a single-mode fiber spool of 20.3 km. The same-length DWDM module is composed of DWDM filters of four different center wavelengths, which are all contained within the transmission spectrum of the CWDM filter. The temporal correlation between the signal photons and the sync signals is analyzed using a TCSPC technique. CH14, CH19, CH24, and CH29: DWDM filters of channels 14, 19, 24, and 29, which have a center wavelength of 1566.31 nm, 1562.23 nm, 1558.17 nm, and 1554.13 nm, respectively.

Next, we conduct an experiment to measure the amount of dispersion induced by a single-mode fiber (G.652.D) of 20.3 km, which is used as the reference dispersive medium to define the amount of dispersion in the DWDM GVD module. Figure 4 depicts the experimental setup for measuring the amount of dispersion induced by the fiber spool. We measure the temporal correlation between the signal photons and the synchronization signals of the pump laser after the signal photons pass through the same-length DWDM module and the fiber spool. Since the same-length DWDM module consists of 100 GHz DWDM filters of four different channels (channels 14, 19, 24, and 29, which have a center wavelength of 1566.31 nm,

1562.23 nm, 1558.17 nm, and 1554.13 nm, respectively) with identical path lengths, the differences between the temporal positions of the measured peaks correspond to the group delay. Thus, we can calculate the dispersion coefficient of the fiber spool as given by [23],

$$\Delta\tau = \mathrm{L}(\Delta\lambda)\mathrm{D}_\lambda, \tag{2}$$

where $\Delta\tau$ represents the temporal full-width at half maximum (FWHM), L denotes the length of the dispersive medium, $\Delta\lambda$ stands for the spectral FWHM, and D_λ denotes the dispersion coefficient in the dispersive medium. In our approach, we used temporal differences between peak positions instead of the temporal FWHM and the spectral spacing between the center wavelengths of DWDM filters instead of the spectral FWHM. Figure 5(a) represents measurement outcomes of the dispersed signal resolved by the same-length DWDM module. The obtained peak positions are analyzed and linearly fitted to determine the group delay of each center wavelength of the DWDM filters, as shown in Fig. 5(b). The dispersion coefficient is assumed to be constant within the spectrum where signal photons are present, yielding $\mathrm{D_s}$ = 17.35 ps/(nm·km). Similarly, for another GVD DWDM module composed of four different DWDM filters which idler photons pass through (channels 33, 38, 43, and 48, which have a center wavelength of 1550.92 nm, 1546.92 nm, 1542.94 nm, and 1538.98 nm, respectively), dispersion coefficient is obtained as $\mathrm{D_i}$ = 16.08 ps/(nm km).

Subsequently, To quantify the amount of dispersion in the DWDM GVD module, we conduct experiments with the same-length DWDM module placed in the path of the signal photons and the fiber spool placed in the path of the idler photons, as shown in Fig. 6. An electrical delay generator is employed to compensate for the temporal delay induced by the fiber spool. Figure 7 presents the experimental results for defining the amount of dispersion in the DWDM GVD module. The red dots represent the coincidence count with both the fiber spool and the same-length DWDM module placed, while the blue dots represent the coincidence count without the DWDM GVD module. Since all paths have the same length, the measured temporal difference of 4.019 ns between channels 14 and 29 is due to the GVD induced by the fiber spool. As we utilize entangled photon pairs with a broad spectrum exceeding 80 nm, the two-photon waveform is determined by the characteristics of the CWDM filter. A discrepancy between the FWHM of the blue dots and the temporal difference (Δt) from the furthest channels is due to the difference between the 3 dB bandwidth of the CWDM filter and the spectral spacing from DWDM channel 14 to

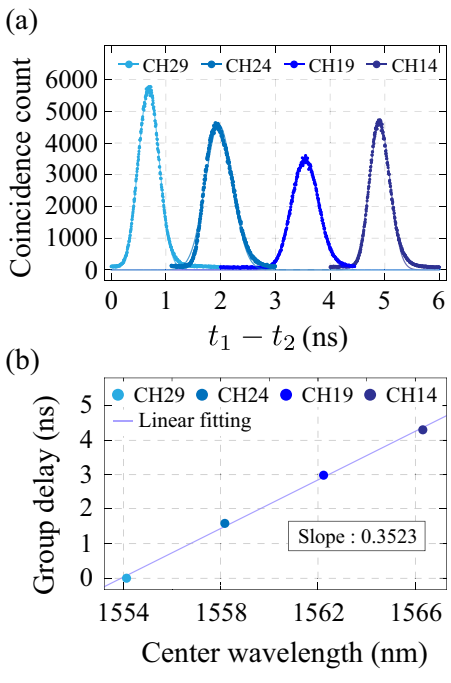

Fig. 5. Experimental results for measuring the amount of dispersion induced by the fiber spool accumulated over 10 minutes. (a) presents a temporal correlation between signal photons and synchronization signal and corresponding Gaussian fitting for each channel of the DWDM GVD module. (b) shows the group delay of photons passing through each of the DWDM filters as a function of the center wavelength of each channel.

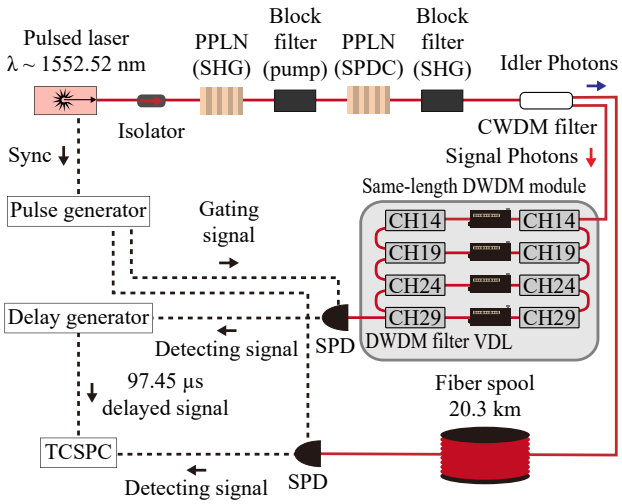

Fig. 6. Experimental setup for defining the amount of dispersion in the DWDM GVD module. The signal photons propagate through the same-length DWDM module, while the idler photons propagate through a 20.3 km fiber spool. The electrical delay of 97.45 μs is introduced to the detection of signal photons to compensate for the temporal delay induced by the fiber spool.

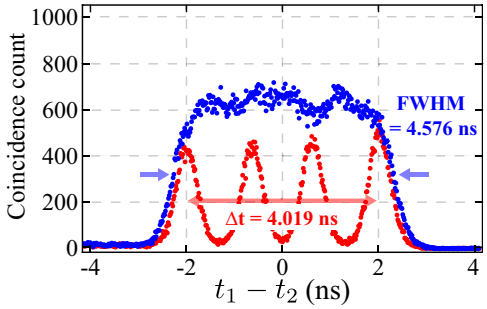

Fig. 7. Experimental results for defining the amount of dispersion in the DWDM GVD module. The data represented by the blue dots corresponds to the coincidence count of entangled photon pairs with the fiber spool in the idler path. The data shown in red represents the coincidence count after adding the same-length DWDM module in the signal path.

channel 29. Additionally, when measuring temporal width, the detector jitter introduces additional uncertainty. However, as the detector jitter solely impacts the width rather than the average value corresponding to the peak position, by removing the jitter effect from the FWHM indicated in blue and dividing by the ratio of the spectral range difference, it is confirmed that it closely corresponds to Δt. In this scenario, designing the DWDM GVD module capable of reproducing the time intervals identical to the measured temporal differences allows for emulating the fiber spool. Through this approach, adjusting the time of flight between signals of DWDM filters makes it possible to effectively induce the intended dispersion by the DWDM GVD module.

Finally, we demonstrate the DWDM GVD module, effectively inducing dispersion by designing consistent path length differences between neighboring paths through the method previously described. The average insertion loss for four different paths of DWDM channels is 4.67 dB, which is measured with the input optical power of 278 μW. Figure 8 illustrates the experimental setup to measure the amount of dispersion in the DWDM GVD module. The DWDM GVD module is engineered to have a temporal difference of 25 ns between neighboring channels, resulting in a temporal difference of 75 ns between the furthest channels. Additionally, coincidence counts are measured with free-running mode to measure temporal correlations beyond the limit of gate width and with a dead time of 50 μs to suppress the afterpulsing effect, unlike in previous experiments. Figure 9 shows the experimental result for measuring the amount of dispersion induced by the DWDM GVD module. The temporal difference between neighboring channels has been set to 24.990 $\pm$ 0.0342 ns, resulting in a temporal difference of 74.970 ns between the furthest channels. Four small peaks, excluding the coincidence count fitted as the Gaussian function marked in red, are the accidental coincidence count measured due to the temporal difference between the furthest channels being longer than the period of the pump laser (approximately 55 ns). Consequently, based on the amount of dispersion induced by optical fiber in Fig. 7, the DWDM GVD module can be analyzed to effectively induce the amount of dispersion equivalent to the optical fiber of 379 km. Furthermore, due to our design ensuring uniform temporal differences between neighboring channels, the DWDM GVD module does not exhibit wavelength-dependent properties, allowing for more precise validation of experiments verifying quantum features utilizing dispersion.

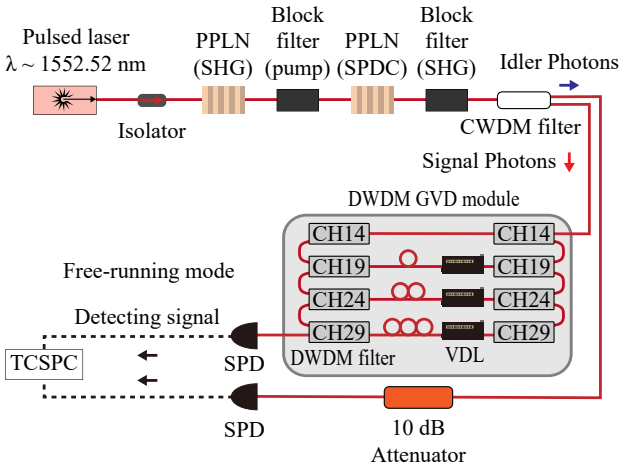

Fig. 8. Experimental setup for measuring the amount of dispersion in the DWDM GVD module. The DWDM GVD module is designed such that the path length of each neighboring DWDM filter differs by 25 ns, using the path length of the DWDM filter of channel 14 as the reference.

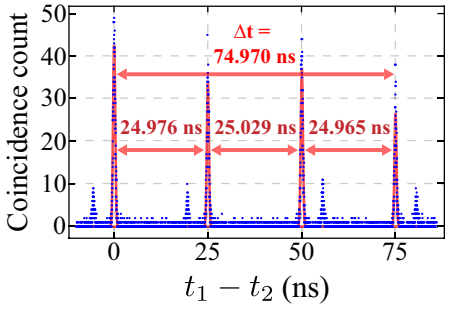

Fig. 9. Experimental result for measuring the amount of dispersion induced by the DWDM GVD module over 1 hour. The blue dots correspond to the measurement result of the coincidence counts of entangled photon pairs with the DWDM GVD module placed in the path of signal photons. The red lines represent Gaussian fittings of the coincidence counts.

IV. Conclusion

In this article, we have proposed the DWDM GVD module, which offers a novel solution for effectively inducing precise and controllable dispersion effects without significant optical loss in fiber systems. We have experimentally demonstrated that the DWDM GVD module, which has the insertion loss of 4.67 dB, is capable of effectively inducing the substantial amount of dispersion equivalent to the single-mode fiber of 379 km. The insertion loss for a typical single-mode fiber of 379 km is 75.8 dB, which is significantly higher than that of our DWDM GVD module. DWDM GVD module for the idler photons, with the same amount of dispersion, is also feasible if a 25 ns interval is maintained between neighboring channels with appropriate channel number (e.g., DWDM filters of channel 33, 38, 43, and 48). Moreover, the versatility of the DWDM GVD module allows manipulation of channel length in reversed order, enabling the straightforward generation of the DWDM GVD module with the dispersion of the opposite sign. In conclusion, we envision that our findings will pave the way for experiments requiring a substantial amount of dispersion or dispersive media exhibiting both positive and negative dispersion characteristics.

References

[1] S. Ranathive, K. V. Kumar, A. N. Z. Rashed, M. S. F. Tabbour and T.V.P. Sundararajan, "Performance signature of optical fiber communications dispersion compensation techniques for the control of dispersion management," *J. Opt. Commu.*, vol. 43, no. 4, pp. 611–623, 2022.

[2] Y.-H. Kim and W. P. Grice, "Measurement of the spectral properties of the two-photon state generated via type II spontaneous parametric downconversion," *Opt. Lett.*, vol. 30, no. 8, pp. 908–910, 2005.

[3] A. Valencia, M. V. Chekhova, A. Trifonov, and Y. Shih, "Entangled two-photon wave packet in a dispersive medium," *Phys. Rev. Lett.*, vol. 88, no. 18, pp. 183601, 2002.

[4] S. Lerch, T. Guerreiro, B. Sanguinetti, P. Sekatski, N. Gisin, and A. Stefanov, "Entanglement, uncertainty and dispersion: a simple experimental demonstration of non-classical correlations," *J. Phys. B: At. Mol. Opt. Phys.*, vol.50, no. 5, pp. 055505, 2017.
[5] K.-H. Hong, S.-Y. Baek, O. Kwon, and Y.-H. Kim, "Dispersive broadening of two-photon wave packets generated via type-I and type-II spontaneous parametric down-conversion," *J. Korean Phys. Soc.*, vol. 73, pp. 1650–1656, 2018.
[6] M. A. Sagioro and S. Pádua, "An optical device for controlling dispersion in quantum communication," *J. Phys. B: At. Mol. Opt. Phys.*, vol. 45, pp. 235502, 2012.
[7] D. Cozzolino, B. D. Lio, D. Bacco, and L. K. Oxenløwe, "High-dimensional quantum communication: benefits, progress, and future challenges," *Adv. Quantum Tech.*, vol. 2, no. 12, pp. 1900038, 2019.
[8] J. Mower, Z. Zhang, P. Desjardins, C. Lee, J. H. Shapiro, and D. Englund, "High-dimensional quantum key distribution using dispersive optics," *Phys. Rev. A*, vol. 87, pp. 062322, 2013.
[9] D. Bunandar, Z. Zhang, J. H. Shapiro, and D. R. Englund, "Practical high-dimensional quantum key distribution with decoy states," *Phys. Rev. A*, vol. 91, pp. 022336, 2015.
[10] M. Y. Niu, F. Xu, J. H. Shapiro, and F. Furrer, "Finite-key analysis for time-energy high-dimensional quantum key distribution," *Phys. Rev. A*, vol. 94, pp. 052323, 2016.
[11] E. B. Treacy, "Optical pulse compression with diffraction gratings," *IEEE J. Quantum Electron.*, vol. 5, no. 9, pp. 454–458, 1969.
[12] F. Salin and A. Brun, J. "Dispersion compensation for femtosecond pulses using high-index prisms," *Appl. Phys.*, vol. 61, no. 10, pp. 4736–4739, 1987.
[13] S.-Y. Baek, Y.-W. Cho, and Y.-H. Kim, "Nonlocal dispersion cancellation using entangled photons," *Opt. Exp.*, vol. 17, no. 21, pp. 19241–19252, 2009.
[14] X. Chen, J. E. Hurley, J. S. Stone, and M.-J. Li, "Chromatic Dispersion Measurements of Single-Mode Fibers, Polarization-Maintaining Fibers, and Few-Mode Fibers Using a Frequency Domain Method," *Photonics*, vol. 10, no. 2, pp. 215, 2023.
[15] N. S. Bergano and C. R. Davidson, "Wavelength division multiplexing in long-haul transmission systems," *J. Lightw. Technol.*, vol. 14, no. 6, pp. 1299–1308, 1996.
[16] P. Goel and R. Kaushik, "Wavelength division multiplexed radio-over-fiber (WDM-RoF) system for next-generation networks with dispersion compensating fiber," *J. Opt. Commun.*, no. 0, 2022.
[17] T. Wasak, P. Szańkowski, W. Wasilewski, and K. Banaszek, "Entanglement-based signature of nonlocal dispersion cancellation," *Phys. Rev. A*, vol. 82, no. 5, pp. 052120, 2010.
[18] J. D. Franson, "Nonlocal cancellation of dispersion," *Phys. Rev. A*, vol. 45, no. 5, pp. 3126, 1992.
[19] G. Brida, M. V. Chekhova, M. Genovese, M. Gramegna, and L. A. Krivitsky, "Dispersion spreading of biphotons in optical fibers and two-photon interference," *Phys. Rev. Lett.*, vol. 96, no. 14, pp. 143601, 2006.
[20] D.-G. Im, Y. Kim, and Y.-H. Kim, "Dispersion cancellation in a quantum interferometer with independent single photons," *Opt. Exp.*, vol. 29, no. 2, pp. 2348–2363, 2021.
[21] J.-H. Kim, J.-W. Chae, Y.-C. Jeong, and Y.-H. Kim, "Long-range distribution of high-quality time-bin entangled photons for quantum communication," *J. Korean Phys. Soc.*, vol. 80, no. 3, pp. 203–213, 2022.
[22] P. Y. Graciano, A. M. A. Martínez, D. Lopez-Mago, G. Castro-Olvera, M. Rosete-Aguilar, J. Garduño-Mejía, R. R. Alarcón, H. C. Ramírez, and A. B. U'Ren, "Interference effects in quantum-optical coherence tomography using spectrally engineered photon pairs," *Sci. Rep.*, vol. 9, no. 9, pp. 8954, 2019.
[23] S.-Y. Baek, O. Kwon, and Y.-H. Kim, "Nonlocal dispersion control of a single-photon waveform," *Phys. Rev. A*, vol. 78, no. 1, pp. 013816, 2008.